Crop Yield Estimation in the Canadian Prairies Using Terra/MODIS-Derived Crop Metrics

Jiangui Liu, Ted Huffman, Budong Qian, Jiali Shang, Qingmou Li, Taifeng Dong, Andrew Davidson, and Qi Jing

***Abstract*—We evaluated the utility of Terra/MODIS-derived crop metrics for yield estimation across the Canadian Prairies. This study was undertaken at the Census Agriculture Region (CAR) and the Rural Municipality (RM) of the province of Saskatchewan, in three prairie agro-climate zones. We compared MODIS-derived vegetation indices, gross primary productivity (GPP), and net primary productivity (NPP) to the known yields for barley, canola, and spring wheat. Multiple linear regressions were used to assess the relationships between the metrics and yield at the CAR and RM levels for the years 2000 to 2016. Models were evaluated using a leave-one-out cross validation (LOOCV) approach. Results showed that vegetation indices at crop peak growing stages were better predictors of yield than GPP or NPP, and EVI2 was better than NDVI. Using seasonal maximum EVI2, CAR-level crop yields can be estimated with a relative root-mean-square-error (RRMSE) of 14–20% and a Nash–Sutcliffe model efficiency coefficient (NSE) of 0.53–0.70, though the exact relationship varies by crop type and agro-climate zone. LOOCV showed the stability of the models across different years, although interannual fluctuations of estimation accuracy were observed. Assessments using RM-level yields showed slightly reduced accuracy, with NSE of 0.37–0.66, and RRMSE of 18–28%. The best performing models were used to map annual crop yields at the Soil Landscapes of Canada (SLC) polygon level. The results indicated that the models could perform well at both spatial scales, and thus, could be used to disaggregate coarse resolution crop yields to finer spatial resolutions using MODIS data.**

***Index Terms*—MODIS, yield, net primary productivity (NPP), gross primary productivity (GPP), EVI2, NDVI.**

I. Introduction

TIMELY and accurate estimates of crop yield are critical for the economic forecasting and risk assessment of agricultural production [1]. Driven by the effects of increasingly frequent extreme weather events on crop yields, and the associated increasing demand for information from stakeholders (producers, grain traders, transporters, and government policymakers) for food security planning, many countries have developed crop monitoring and yield forecasting systems to provide regional, national, and global production outlooks for major field crops [2], [3]. In Canada, while historical yield data are available and used in several national programs [4], [5], the only consistent yield data are available at the broad scale of Census Agricultural Regions (CAR). It is obtained through a farm survey program by Statistics Canada, the official federal government statistical reporting agency for Canada. Estimates of crop yields at more detailed regional and local scales are needed to better support the aforementioned national research and operational programs.

Crop yield is determined by many factors such as soil conditions, temperature, soil moisture, and management practices [6]–[8]. These factors are reflected by crop growth conditions that can be characterized with crop biophysical and biochemical parameters, such as vegetation cover fraction, green leaf area index (LAI), and fraction of absorbed photosynthetically active radiation (fAPAR). Remote sensing can be used to measure these parameters continuously in space and time [9]–[12], thus providing a useful tool for yield estimation. The availability of free data in near real time from some satellite sensors (e.g., MODIS and AVHRR) allows for within-season yield forecasts with relatively lower cost [2].

Three general types of approaches can be identified in using remote sensing data to estimate crop yields. The first type of approach is to correlate grain yield with vegetation indices obtained at a single date or integrated over a period of time during a growing season, to map spatial variability of final yield [13]–[15]. Many vegetation indices are well correlated with biophysical parameters indicative of biomass accumulation [9]–[12]. Of these, the normalized difference vegetation index (NDVI)—which uses red and near infrared reflectances—has received much attention because of its computational simplicity and its use in long term satellite data records (e.g. AVHRR). However, NDVI is shown to be prone to saturation at high levels of aboveground biomass. To directly address this issue, Huete *et al.* [16], [17] developed the enhanced vegetation index (EVI). The EVI, which uses blue, red, and near infrared reflectances, is resistant to the effect of atmospheric aerosols and more sensitive to canopy structural variations at high biomass conditions than the NDVI. This index is included as a standard Level-3 MODIS vegetation index product. The desire to calculate the EVI back in time to the AVHRR data records, in the absence of a blue band, prompted the development of a two-band version of the EVI (EVI2) based on the red and near infrared reflectances only

Manuscript received December 13, 2019; revised March 4, 2020; accepted March 23, 2020. Date of publication May 29, 2020; date of current version June 11, 2020. This work was supported in part by Agriculture and Agri-Food Canada through the Bio-product project (J-001589), in part by the Nutrient run-off and soil health (J-002264), and in part by the Sustainability Metrics project (J-002316). *(Corresponding author: Jiangui Liu.)*

Jiangui Liu, Ted Huffman, Budong Qian, Jiali Shang, Taifeng Dong, Andrew Davidson, and Qi Jing are with the Science and Technology Branch, Agriculture and Agri-Food Canada, Ottawa, ON K1A 0C6, Canada (e-mail: jiangui.liu@canada.ca; ted.huffman@canada.ca; budong.qian@canada.ca; jiali.shang@canada.ca; taifeng.dong@canada.ca; andrew.davidson2@canada.ca; qi.jing@canada.ca).

Qingmou Li is with the Canadian Hazards Information Service (CHIS), Natural Resources Canada, Ottawa, ON K1A 0Y3, Canada (e-mail: qingmou.li@canada.ca).

Digital Object Identifier 10.1109/JSTARS.2020.2984158

This work is licensed under a Creative Commons Attribution 4.0 License. For more information, see https://creativecommons.org/licenses/by/4.0/

[18]. The EVI2 is applicable to sensors that lack a blue band (such as MODIS at 250 m).

In an agricultural context, Becker–Reshef *et al.* [19] used MODIS seasonal maximum NDVI to develop a generalized empirical approach for winter wheat yield estimation at a regional scale. Mkhabela *et al.* [15] used time-series 10-day composite MODIS NDVI for crop yield estimation at the CAR-level in the Canadian Prairies, and found that the best time for yield estimation was dependent on crop and agro-climate zones. Bolton and Friedl [20] tested MODIS time-series NDVI, EVI2, and NDWI (the normalized difference water index [21]), and found that performance for yield estimation was improved using phenologically adjusted vegetation indices. While these studies rely on the short revisit cycles of moderate resolution satellite sensors (e.g., AVHRR, MODIS) to capture crop seasonal dynamics, they have been limited to regional applications because of the relatively coarse pixel resolution of the data. Other studies have fused coarse and fine spatial resolution satellite data to generate synthetic datasets with both high spatial and high temporal resolutions [13], [22], [23].

The second approach uses radiation-use efficiency models, where crop biomass or yield is related to gross or net primary productivity, which are modeled using crop parameters estimated from remote sensing data, agro-meteorological data, and some crop-specific parameters [24]–[27]. These methods are often used to model carbon cycling in the biosphere using satellite observations [28]–[30]. In this approach, fAPAR is estimated from remote sensing data, and light-use efficiency (LUE) is determined as the product of maximum radiation-use efficiency and factors representing environmental stresses, such as water stress and heat stress.

The third approach relies on the assimilation of remotely sensed data into process-based crop models [31], [32] or mechanistic radiation use efficiency models [22], [33]. Satellite-derived crop parameters such as LAI or fAPAR are compared with state variables (variables used to characterize crop growth dynamics) in the models, either to reinitialize certain model parameters or to update the state variables. The advantage of this approach is that the spatiotemporal variability of land surface conditions captured from space is integrated with physically based process models to improve model performance. Operational implementation of this approach over large regions is often challenging because of its high computational overhead and the need for large number of cultivar-specific parameters [31], whereas the first two approaches are simple, straightforward, and effective to be applied at large scales.

The Canadian Crop Yield Forecaster (CCYF) was developed at Agriculture and Agri-Food Canada (AAFC) to provide within-season yield forecasts during the growing season [2]. The CCYF is a probabilistic model that integrates climate data, EO-based vegetation indices, and soil and crop information using a soil water budget model and statistical algorithms. While the CCYF is able to deliver yield forecasts with good accuracy, it is limited by its application at coarse spatial resolutions (i.e., the CAR and provincial scales [1]). To directly address this limitation and better fulfill the operational yield forecasting needs, an approach is needed for yield estimation at finer spatial resolutions. To this end, the objectives of our study were to, first, evaluate the potential of satellite-derived metrics for crop yield estimation in the Canadian Prairies, and second, establish models for yield estimation at different spatial resolutions for the purpose of providing a robust approach for operationally generating long term historical yield databases. To do this, we intend to map major crop yields at the Soil Landscapes of Canada (SLC) level, because: 1) It is the lowest level in the Canadian ecological stratification system [34], 2) it is used as the basis for several regional and national programs, such as agro-environmental assessment, and 3) yield is not generally spatially available at this level. There are totally 1434 SLC polygons in the study area. Several remote sensing metrics based on MODIS land products were assessed, including vegetation indices derived from the 250-m reflectance, the gross primary productivity (GPP) and the net primary productivity (NPP).

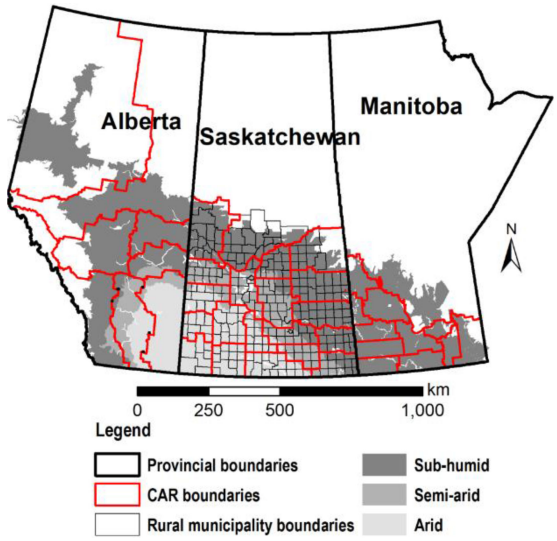

Fig. 1. Canadian Prairie agricultural region, with Provincial boundaries outlined in black, Census Agricultural Regions (CAR) in red, and the rural municipalities of Saskatchewan in gray. The shaded areas are croplands in the three agro-climate zones (subhumid, semiarid, and arid).

II. Materials and Methods

A. Study Area

Our study covers the Canadian prairie provinces of Alberta (AB), Saskatchewan (SK), and Manitoba (MB). The region is characterized by a continental climate with cold winters and hot summers, and comprises three agro-climatic zones (subhumid, semiarid, and arid; Fig. 1). The growing season lasts from mid-April to the end of September. Crops are susceptible to drought conditions due to the relatively low annual precipitation of about 454 mm, which peaks in June and July [35]. The soils in the region are dominated by brown grassland soils in the arid zone, dark-brown mixed grassland soils in the semiarid zone, and black and gray wooded soils in the subhumid zone. About 80% of Canada's total cropland area is in this region.

B. Crop Yield Data

In Canada, information on annual crop yield is available at various spatial scales. CAR-level yields are collected by

Statistics Canada through a rigorous farm survey program[1]. This program records seeded and harvested areas, crop yields and production on an annual basis for most principal field crops, and some specialty crops. This provides the most geographically complete and consistent source of long term crop yield data in Canada. While more spatially detailed county-level yields are compiled and held by provincial agencies, they may be absent for some provinces, inconsistent in terms of the crops and/or years reported, and/or publicly unavailable.

There are a total of 40 CARs in the three Canadian Prairie provinces (8 in AB, 20 in SK, and 12 in MB) (Fig. 1). The CARs are ascribed to subhumid (25), semiarid (7), and arid (8) zones based on the majority of the area of each CAR. RM-level crop yields in SK are collected and maintained by the provincial government. These records are readily available with few gaps. There are a total of 295 RMs in the province (137 in the subhumid zone, 78 in the semiarid zone, and 80 in the arid zone). For this study, we obtained yields of three major crops (barley, canola, and spring wheat) at the CAR- and RM-levels for the years 2000 through 2016, as outlined in Fig. 1.

C. MODIS Data

MODIS land products were retrieved from the Land Processes Distributed Active Archive Center (LP DAAC)[2]. The following products were obtained.

1) The 250-m resolution 8-day composite surface reflectance product (MOD09Q1, Collection-5). This product was used to derive time series of the NDVI and EVI2. The EVI2 has been shown to perform better than NDVI in reducing atmospheric effects and is less likely to saturate over areas of high vegetation productivity [12], [36]. The MOD09Q1 product was used because it has a finer temporal resolution than the 16-day MODIS standard vegetation index product (MOD13Q1).
2) The 500-m resolution gross primary productivity product (GPP, MOD17A2H, Collection-6). This product consists of a cumulative 8-day composite of GPP and net photosynthesis (PSN) generated using the Biome-BGC ecosystem model [37] and a light-use efficiency concept [38]. The algorithm incorporates the MODIS LAI/fAPAR product (MOD15), estimated PAR, and surface meteorological data (GMAO/NASA) using a set of biome-specific radiation use efficiency parameters obtained from the Biome properties look-up table (BPLUT). Specifically, fAPAR is used to calculate light absorption (APAR), and LAI is used to derive maintenance respiration of leaf (r_{ml}) and fine root (r_{mr}). The realized light-use efficiency (ε) is calculated as biome-specific maximum light-use efficiency $\varepsilon_{\max}$ down regulated by temperature ($f(\mathrm{T})$) and water vapor pressure ($f(\mathrm{VPD})$) stress factors derived from meteorological data. In the MODIS Net Primary Productivity (NPP) algorithm, the annual growth respiration (r_{g}) was considered as 25% of the annual NPP. More details about the algorithm can be found in Running and Zhao [39], [40] and Zhao *et al.* [41]. GPP and NPP are calculated as

$$\begin{aligned}\mathrm{GPP} &= \varepsilon * \mathrm{APAR} \\ &= \varepsilon_{\max} * f(\mathrm{T}) * f(\mathrm{VPD}) * f\mathrm{APAR} * \mathrm{PAR} \quad (1)\end{aligned}$$

$$\mathrm{NPP} = \mathrm{GPP} - r_{\mathrm{ml}} - r_{\mathrm{mr}} - r_{\mathrm{g}}. \quad (2)$$

The study area is covered by six MODIS tiles (h10v03, h11v03, h12v03, h10v04, h11v04, and h12v04). Annually, there are 46 sets of 8-day composites of reflectance and GPP/NPP products. For subsequent processing, the six tiles were mosaicked using the MODIS Reprojection Tool (MRT, Release 4.1) without reprojection.

D. MODIS Data Processing

To support the analysis for crop yield estimation, CAR-level and RM-level MODIS data were extracted using a cropland mask, projected to the same sinusoidal projection used in the MODIS products. The MODIS sinusoidal projection was used to avoid the computational overhead of reprojecting thousands of MODIS tiles. MODIS data processing was carried out following to the following steps.

1) *Creation of a Cropland Mask:* We derived the cropland mask from 30-m resolution Canadian decadal (circa-1990/2000/2010) land-use maps[3]. These maps use the legend classification of the Intergovernmental Panel on Climate Change (IPCC). The maps were created from as many relevant digital maps and information sources as possible using a weight of evidence approach, through which the "most probable" land use class of each pixel was determined [42]. The overall mapping accuracy of these datasets is greater than 95%. The 30-m land use maps were reprojected to the sinusoidal coordination system, and then resampled to 250- and 500-m grids to match the projection and pixel resolution of the MODIS products used in this study.
2) *Screening Pixels Using MODIS Quality Control (QC) Indicators*: To ensure that only the highest quality MODIS retrievals were used in this study, only pixels identified as free from cloud and cloud shadow contamination were retained for analysis.
3) *Extraction of Vegetation Indices*: High-quality cropland pixels were identified in each MODIS image, from which the red and near-infrared reflectances were used to calculate CAR- and RM-level average NDVI and EVI2.
4) *Extraction of GPP/NPP Data*: Time-series CAR- and RM-level average GPP and PSN were generated using the high-quality cropland pixels. Annual GPP and PSN were calculated by integrating the time-series GPP and PSN over the typical crop growth cycle from mid-April to the end of September. Annual NPP was calculated by subtracting annual growth respiration from the cumulative PSN. Annual GPP was calculated as the sum of time-series GPP within the growing period.

[1][Online]. Available: https://www150.statcan.gc.ca/
[2][Online]. Available: https://lpdaac.usgs.gov/
[3][Online]. Available: https://open.canada.ca/data/en/dataset/18e3ef1a-497c-40c6-8326-aac1a34a0dec

The above steps produced the following four MODIS metrics for use in this study: 1) Time-series NDVI and EVI2; 2) maximum NDVI and EVI2; 3) maximum GPP; 4) annual GPP and NPP.

E. Modeling the Relationships Between MODIS Metrics and Crop Yields

A linear relationship is assumed to relate MODIS metrics with crop grain yields [13], [14], [20] although nonlinear models have also been attempted [15]. A multiple linear regression model is used here

$$Y = \mathrm{a}_1 X + \mathrm{a}_2 t + \mathrm{a}_0 \tag{3}$$

where X represents a MODIS metrics, t represents the specific year to account for long term yield increases due to agronomic technology, and Y is crop yield. In consideration of crop responses to different environmental conditions, regression analyses were conducted independently for the three agro-climate zones. Our intention was to develop yield estimation models to disaggregate CAR-level yields to finer spatial scales at the RM-level (Saskatchewan) or the SLC-level (prairies). Thus, CAR-level yields were used to develop the models, and RM-level yield was used to assess model performance in revealing the spatiotemporal variability of crop productivity. We also adopted a leave-one-out cross-validation (LOOCV) approach to assess model robustness at the CAR-level by iteratively excluding the yields of a given year in model development and then testing model performance using the actual yields of that year for validation.

F. Model Assessment

The Nash–Sutcliffe model efficiency coefficient (NSE), the root-mean-square-error (RMSE) and the relative RMSE (RRMSE), defined in (4)–(6) below, were used to assess model performance

$$\mathrm{NSE} = 1 - \sum_{i=1}^{n} \left(Y_{\mathrm{oi}} - Y_{\mathrm{ei}}\right)^2 / \sum_{i=1}^{n} \left(Y_{\mathrm{oi}} - \bar{Y}_{\mathrm{o}}\right)^2 \tag{4}$$

$$\mathrm{RMSE} = \sqrt{\sum\nolimits_{\mathrm{i}=1}^{\mathrm{n}} \left(\mathrm{Y_{oi}} - \mathrm{Y_{ei}}\right)^2 / \mathrm{n}} \tag{5}$$

$$\mathrm{RRMSE} = 100\ RMSE/\bar{Y}_o \tag{6}$$

where Y_{o} and Y_{e} are the reported and estimated yields, respectively, $\bar{Y}_{\mathrm{o}}$ is the mean of reported yields, n is the number of samples, and the subscript i represents individual samples. The definition of NSE in this study follows the recommendation of Kvålseth [43], and is not the squared linear correlation coefficient. To assess each model, we compared the performance of each MODIS metric for CAR-level yield estimation. To do this, we established multiple linear regression models to estimate yield at CAR-level and then assessed model robustness and applicability. This was done by: 1) Applying a LOOCV at the CAR-level to assess interannual variation, and 2) using RM-level yields to assess the effects of spatial scaling. We then applied the established model to map the spatial variability of crop yields at the SLC-level.

III. Results

A. Time-Series Vegetation Indices

The correlation between time series of the two vegetation indices and crop yields at the CAR-level showed clear seasonal patterns. Fig. 2 shows the NSE of the three crops in the three agro-climate zones, as functions of the day-of-year (DOY) of each MODIS 8-day composite. These results were obtained from multiple linear regression models using data from all 17 years used in the study. We also applied a running average to the original time-series data for comparative purposes, using the period covered by three composites (24 days). The NSE curves are shown as NDVI_a and EVI2_a in Fig. 2.

For all cases, NSE increased from the start of the growing season to a maximum in the mid-season, and then decreased to the end of the season. The time to reach maximum NSE changed among crops and agro-climate zones (between DOY of 185 and 209). While the NSE of EVI2 was higher than that of NDVI for most cases, it reached its maximum at about the same time as the NDVI. The difference in NSE was smallest in the arid zone. NSE was improved by using the running average. During the mid-season, the semiarid zone had the strongest correlation. In the arid zone, the change in NSE from the beginning of the season to the mid-season was the smallest.

B. Comparison of Correlations Between MODIS Metrics and Crop Yields

Fig. 3 provides a comparison of NSE between different MODIS metrics, including the best regression model using running averaged time-series NDVI and EVI2, the maximum NDVI and EVI2 (Max NDVI and Max EVI2), the maximum GPP, and annual GPP and NPP. Here, the best regression models using the two vegetation indices were considered as the ones having the largest NSE in a growing season for each crop in each agro-climate zone. For the models based on maximum NDVI, EVI2, or GPP, the maximum values for different CARs were often from different composites.

For the two vegetation indices, it was observed that NSE values obtained from the best regression model of the time-series data are comparable with those derived from the model based on the maximum value of vegetation indices. The performance of EVI2 was better than that of the NDVI in the subhumid and semiarid zones, but comparable in the arid zone. The GPP and NPP metrics showed a lower NSE than the vegetation indices. The performance of models using the annual GPP and NPP were comparable for all cases, but were inferior to the models using the seasonal maximum GPP in most cases.

C. Crop Yield Estimation at the CAR-Level

Based on the results presented in the previous section, regression models for yield estimation were developed using maximum EVI2, maximum NDVI, and annual NPP. We chose to use maximum vegetation indices as the predictor variable

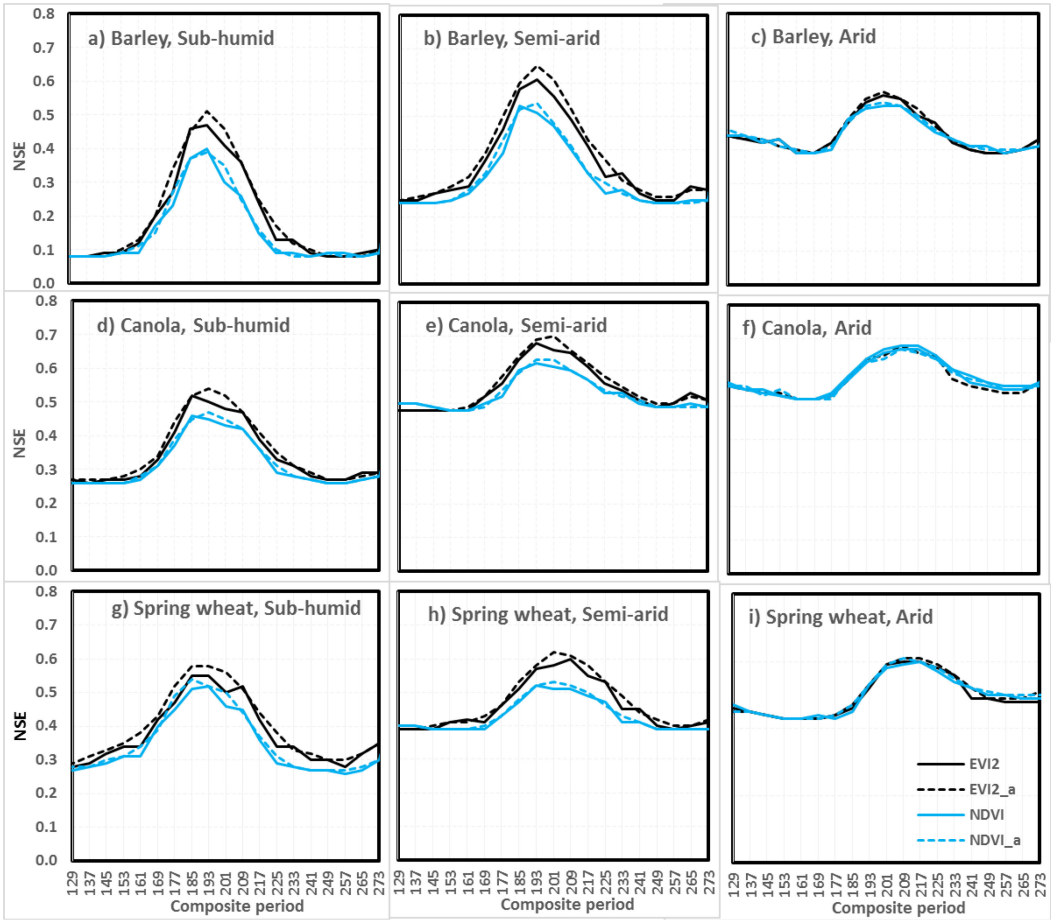

Fig. 2. Nash–Sutcliffe model efficiency coefficient (NSE) between crop yields at the CAR-level and MODIS vegetation indices (2000–2016) as a function of composite days. Solid lines represent the original vegetation indices, and dashed lines (EVI2_a and NDVI_a) represent the moving average of three composites.

because they showed comparable performance with the best regression models using time-series vegetation indices. Although annual NPP (and annual GPP) had a lower NSE than maximum GPP, it was selected for comparison with vegetation indices because crop respiration cost was subtracted from GPP. Since instantaneous GPP is directly controlled by fAPAR, which is largely determined by vegetation indices such as NDVI [39], [40], annual NPP may be a more independent physical quantity than GPP in this case. Fig. 4 compares the reported and estimated CAR-level yields over the 17 years, and Table I lists the regression results.

As shown in Fig. 3, EVI2 had the best performance for yield estimation in all cases, with the range of NSE falling between 0.53 for barley (in the arid zone) and 0.70 for canola (in the semiarid zone). Annual NPP had the lowest NSE, which fell between 0.08 for barley (in the subhumid zone) and 0.59 for canola (in the arid zone). The range of NSE for NDVI fell between 0.42 for barley (in the subhumid zone) and 0.62 for canola (in the semiarid and arid zone). RMSE was generally lowest for canola (253–381 $\mathrm{kg\ ha^{-1}}$), and highest for barley (385–664 $\mathrm{kg\ ha^{-1}}$). The RRMSE values for the three crops were between 15% and 22%. Fig. 4 shows an overestimation for low yields and an underestimation for high yields using the three metrics. EVI2 showed the least tendency and annual NPP the most tendency for this bias.

D. Assessment of Crop Yield Estimation

To further assess model performance using the three MODIS metrics, we inspected the annual variation of RRMSE obtained through the LOOCV using CAR-level yield data (Fig. 5). RRMSE for each year was obtained using the regression model established using crop yields from all other years. For comparison, annual RRMSE was also obtained using the regression model established using yields from all 17 years (all-data model). RRMSE obtained through LOOCV was similar to that obtained using the all-data models. With the exception of canola in the arid zone, RRMSE for the three crops using EVI2 ranged between 6% and 30%. In most cases, the annual RRMSE for EVI2 was lower than for NDVI, although the difference was not large. RRMSE for annual NPP was higher than that for the two vegetation indices.

Poor yield estimation was observed in several years, as shown by the upward spikes in the annual variation of RRMSE in Fig. 5. Using EVI2 as a predictor, the larger error was observed throughout 2007 for all but one crop in all agro-climate zones

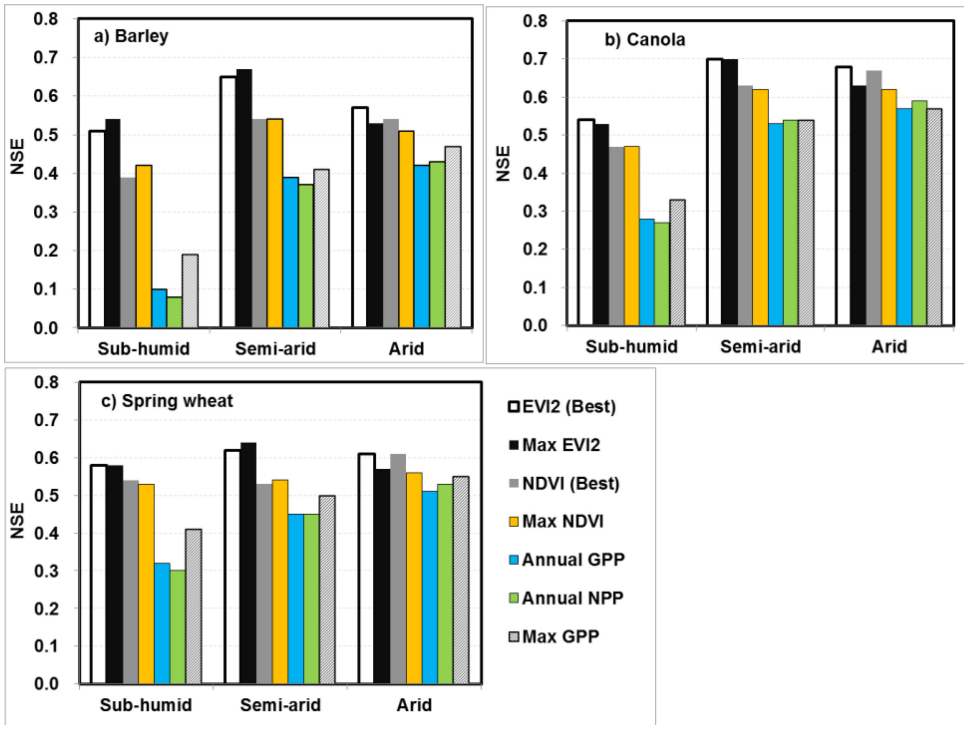

Fig. 3. Comparison of the Nash–Sutcliffe model efficiency coefficient (NSE) between crop yields and MODIS crop metrics. GPP, gross primary productivity; NPP, net primary productivity; "Max" represents the maximum value in the time-series composite data in a growing season.

TABLE I
RESULTS OF MULTIPLE LINEAR REGRESSION MODELS FOR YIELD ESTIMATION

Crop	Zone	Yield/CV(%)/n	Metric	a1	a2	a0	RMSE	RRMSE (%)	NSE	r1	r2
Barley	Sub-humid	3137	EVI2	9730	33.5	-2147	472	15	0.54	0.69	0.29
		/ 22	NDVI	10284.4	39.3	-4769	528	17	0.42	0.59	0.29
		/ 421	NPP	882.5	36.3	2491	664	21	0.08	0.18	0.29
	Semi-arid	2733	EVI2	8794.7	18.5	-1503	385	14	0.67	0.81	0.49
		/ 25	NDVI	7114.8	28.4	-2314	457	17	0.54	0.71	0.49
		/ 119	NPP	8719.7	11.2	-188	534	20	0.37	0.61	0.49
	Arid	2468	EVI2	4762.5	41.3	330	431	17	0.53	0.68	0.62
		/ 26	NDVI	3589.8	43.7	59	441	18	0.51	0.66	0.62
		/ 136	NPP	3743.9	55.3	1043	476	19	0.43	0.58	0.63
Canola	Sub-humid	1765	EVI2	4786.2	43.3	-1051	306	17	0.53	0.55	0.51
		/ 25	NDVI	5153.3	46.1	-2410	326	18	0.47	0.46	0.51
		/ 425	NPP	1114.9	41.6	982	381	22	0.27	0.33	0.51
	Semi-arid	1647	EVI2	4289	41.7	-680	253	15	0.70	0.74	0.69
		/ 28	NDVI	3344.8	47.2	-996	284	17	0.62	0.65	0.69
		/ 119	NPP	3839.3	40.8	74	315	19	0.54	0.67	0.69
	Arid	1571	EVI2	3483.5	48.5	-149	314	20	0.63	0.71	0.72
		/ 33	NDVI	2737.8	49.3	-405	318	20	0.62	0.70	0.72
		/ 134	NPP	4003.9	49.7	115	331	21	0.59	0.69	0.72
Spring wheat	Sub-humid	2806	EVI2	8409.5	67.7	-2041	454	16	0.58	0.61	0.50
		/ 25	NDVI	9319.3	73.0	-4627	481	17	0.53	0.53	0.50
		/ 379	NPP	3961.9	54.8	796	589	21	0.30	0.44	0.50
	Semi-arid	2339	EVI2	6263.1	45.8	-939	379	16	0.64	0.74	0.62
		/ 27	NDVI	4739.3	54.7	-1309	428	18	0.54	0.63	0.62
		/ 119	NPP	5494.1	45.2	193	469	20	0.45	0.63	0.62
	Arid	1978	EVI2	3677.7	37.3	320	311	16	0.57	0.70	0.66
		/ 24	NDVI	2872.1	37.2	65	313	16	0.56	0.70	0.66
		/ 122	NPP	4184.8	39.1	597	327	17	0.53	0.67	0.66

Yield $(\mathrm{kg/ha})$, CV, and n are average of observed yield, coefficient of variation of yield, and the number of samples in an Agro-Climate Zone, respectively; $a1$, $b2$, $and\ a0$ are regression coefficients correspondent to Eq. (3); RMSE $(\mathrm{kg/ha})$ is the root-mean-square-error; RRMSE is RMSE relative to average observed yield; NSE is the Nash–Sutcliffe model efficiency coefficient; $r1$ and $r2$ are linear correlation coefficients for the metric and for the year, respectively.

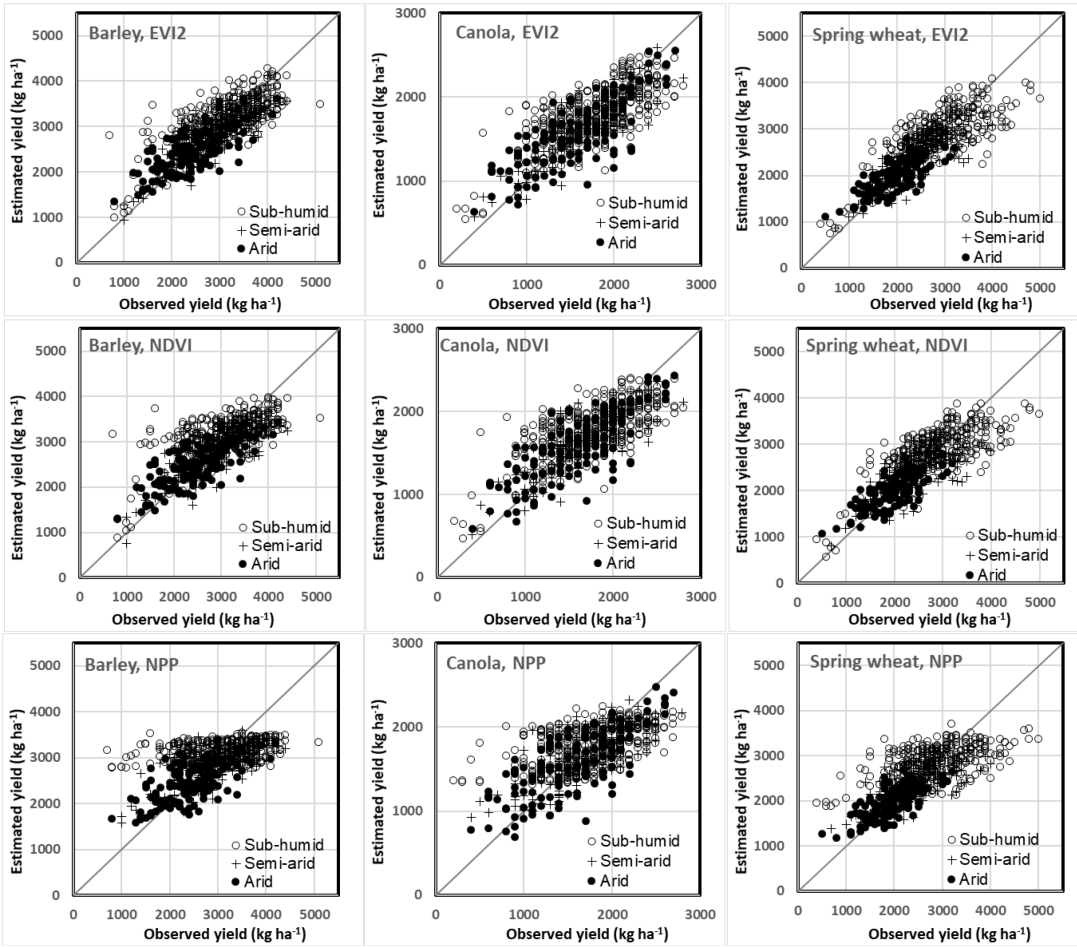

Fig. 4. Comparison of measured and estimated CAR-level crop yields, using multiple linear regression models established with yield data from all years.

TABLE II
MODEL PERFORMANCE ASSESSED USING SASKATCHEWAN RURAL MUNICIPALITY (RM) YIELDS

Crop	Zone	n	Yield	CV%	EVI2			NDVI			Annual NPP		
					NSE	RMSE	RRMSE %	*NSE*	RMSE	RRMSE %	*NSE*	RMSE	RRMSE %
Barley	Sub-humid	2285	2919	26	0.49	536	18	0.43	566	19	0.06	726	25
	Semi-arid	1294	2552	29	0.49	531	21	0.45	551	22	0.29	629	25
	Arid	1295	2343	31	0.24	632	27	0.21	645	28	0.13	676	29
Canola	Sub-humid	2304	1629	29	0.51	332	20	0.49	338	21	0.35	383	24
	Semi-arid	1305	1542	33	0.66	297	19	0.61	317	21	0.50	359	23
	Arid	1154	1483	39	0.48	410	28	0.46	419	28	0.40	443	30
Spring wheat	Sub-humid	2309	2488	27	0.47	485	20	0.46	491	20	0.29	560	23
	Semi-arid	1320	2149	30	0.62	396	18	0.58	420	20	0.44	484	23

N: Number of samples; yield $(\mathrm{kg\,ha^{-1}})$ and CV are average and coefficient of variation of measured yield, respectively; NSE: The Nash–Sutcliffe model efficiency coefficient; RMSE $(\mathrm{kg\,ha^{-1}})$: Root-mean-square-error; RRMSE: RMSE relative to mean measured yield.

(the exception was barley in semiarid zone). Large errors were also observed in 2012 (for canola and barley), and a period between 2001 and 2004 (with variation in the specific year among crops and agro-climate zones). For barley, the largest RRMSE was 19% in the subhumid zone in 2001, 20% in the semiarid zone in 2002, and 23% in the arid zone in 2003. For canola, the largest RRMSE was 28% in the subhumid zone in 2004, and 24% and 57% in 2003 in the semiarid and arid zones, respectively. For spring wheat, the largest RRMSE was 22% in the arid zone in 2002, and 25% and 23% in 2001 in the subhumid and the semiarid zones, respectively.

An assessment of model performance was also conducted using Saskatchewan RM-level yields. Fig. 6 shows the comparison between reported and estimated yields, and Table II provides statistics for yield estimation using EVI2, NDVI, and annual NPP. The scatter-plots in Fig. 6 are similar to the CAR-level data

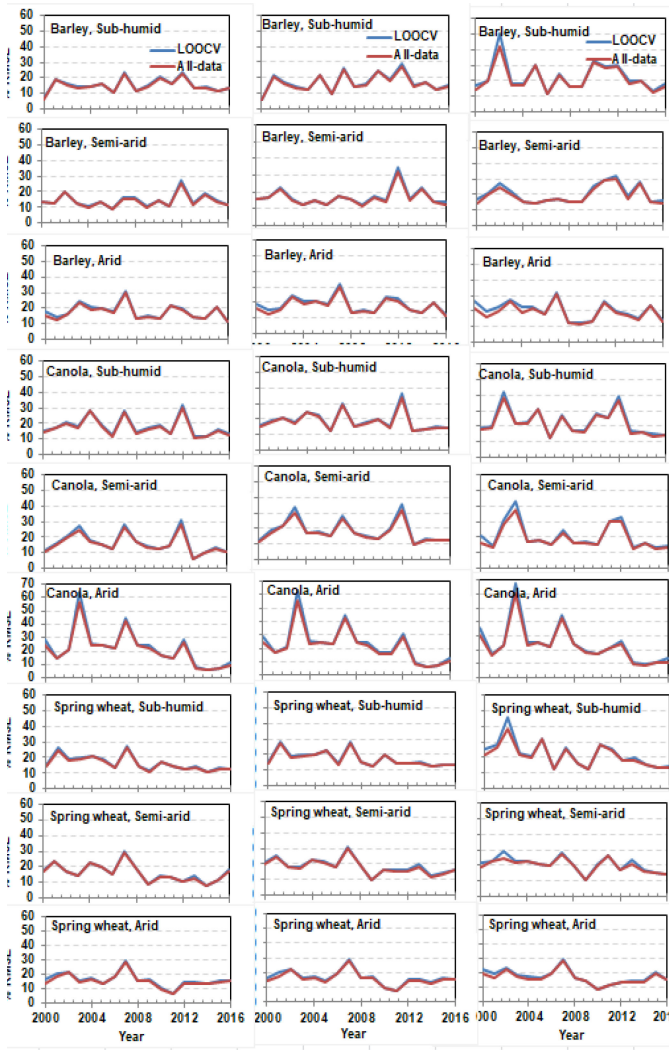

Fig. 5. RRMSE obtained from leave-one-out cross validation using CAR-level yield data (LOOCV, blue lines), as compared with that obtained from regression models using yields from all years (All_data, red lines). Left, middle, and right columns are for EVI2, NDVI, and annual NPP, respectively.

shown in Fig. 4. NDVI showed a stronger tendency of overestimation at low yields and underestimation at high yields than EVI2. Annual NPP was poor for yield estimation, particularly for barley in the subhumid zone. Table II shows that, for each crop in each zone, RRMSE was the lowest using models with maximum EVI2 as predictor. The largest RRMSE values were found in the arid zone for the three crops.

E. Mapping Crop Yield at the SLC Level

Since maximum EVI2 performed better than maximum NDVI and annual NPP, the multiple linear regression models based on maximum EVI2 were used to map annual crop yields for SLC polygons over the study period. Fig. 7 shows maps of the estimated yields for the three crops in 2000 (left) and 2016 (right). Crop yields of SLC polygons were highest in the subhumid zone and lowest in the arid zone. Within-zone variability of estimated SLC level yields is also observable. Crop yields increased markedly over the 17 years, with annual fluctuations within each climate zone shown in Fig. 8. Average yields of barley in the subhumid, semiarid, and arid zones increased from 3305, 2428, and 2114 $\mathrm{kg\ ha^{-1}}$ to 3965, 3588, and 3405 $\mathrm{kg\ ha^{-1}}$, respectively. Canola yields increased from 1631, 1237, and 1156 to 2385, 2325, and 2393, respectively, and spring wheat yields increased from 2671, 1860, and 1698 to 3862, 3208, and 2782 $\mathrm{kg\ ha^{-1}}$ in the three zones, respectively. The increase in estimated yield over the study period ranges from 50 to 82 $\mathrm{kg\ ha^{-1}yr^{-1}}$ for barley, 52 to 73 $\mathrm{kg\ ha^{-1}yr^{-1}}$ for canola, and 63 to 91 $\mathrm{kg\ ha^{-1}yr^{-1}}$ for spring wheat. These long term rates of increase in crop yields are comparable to the rates calculated from reported yields at the CAR-level (data not shown).

IV. Discussion

A. Cropland Mask

A general cropland mask was used to facilitate the identification of high quality MODIS retrievals over cropland. This mask was derived from 30-m land use maps which did not discriminate different crops. As a result, crop-specific growth conditions could not be captured from the time-series MODIS data used here. However, this is likely not a limitation for our study because the majority of crops grown within the study region are spring seeded, and show similar growth cycles. The implementation of the AAFC Annual Space-Based Crop Inventory for the prairies in 2009 and nationally in 2011 [44] means that, crop-specific masks could be used to further test the yield estimation procedures developed in this article. However, the evaluation of the use of such masks for yield forecasting across Canada by Zhang *et al.* [1] showed that their use improved yield forecasts in less than half of the CARs in the Prairie Provinces. This likely indicates the comparable values of vegetation indices among different crops. Nevertheless, even though crop specific masks cannot be generated for the Canadian Prairies before 2009, a yield estimation model based on a general cropland mask might still be useful for generating an historical crop yield database.

B. Time-Series Vegetation Indices

Several studies have shown the effectiveness of using vegetation indices for crop yield estimation, and the most effective indices for this purpose are derived from the peak growth stage [13]–[15], [20], [27]. One reason for this is that vegetation indices indicate crop photosynthetic capacity and are proportional to the aboveground live biomass accumulated by plants through the integration of growth resources and constraints. The amount of green biomass accumulated up to the peak growing stage is proportional to the maximum photosynthetic capacity in a growing season, and thus, largely determines final biomass accumulation and grain yields. However, vegetation indices at the peak growing stage do not capture crop conditions later in the season. As a result, final grain yields may be impacted by abnormal growth conditions occurring after the peak growing stage. Integrating conditions (e.g., climate variability) after the peak growing stage could improve the performance of yield models.

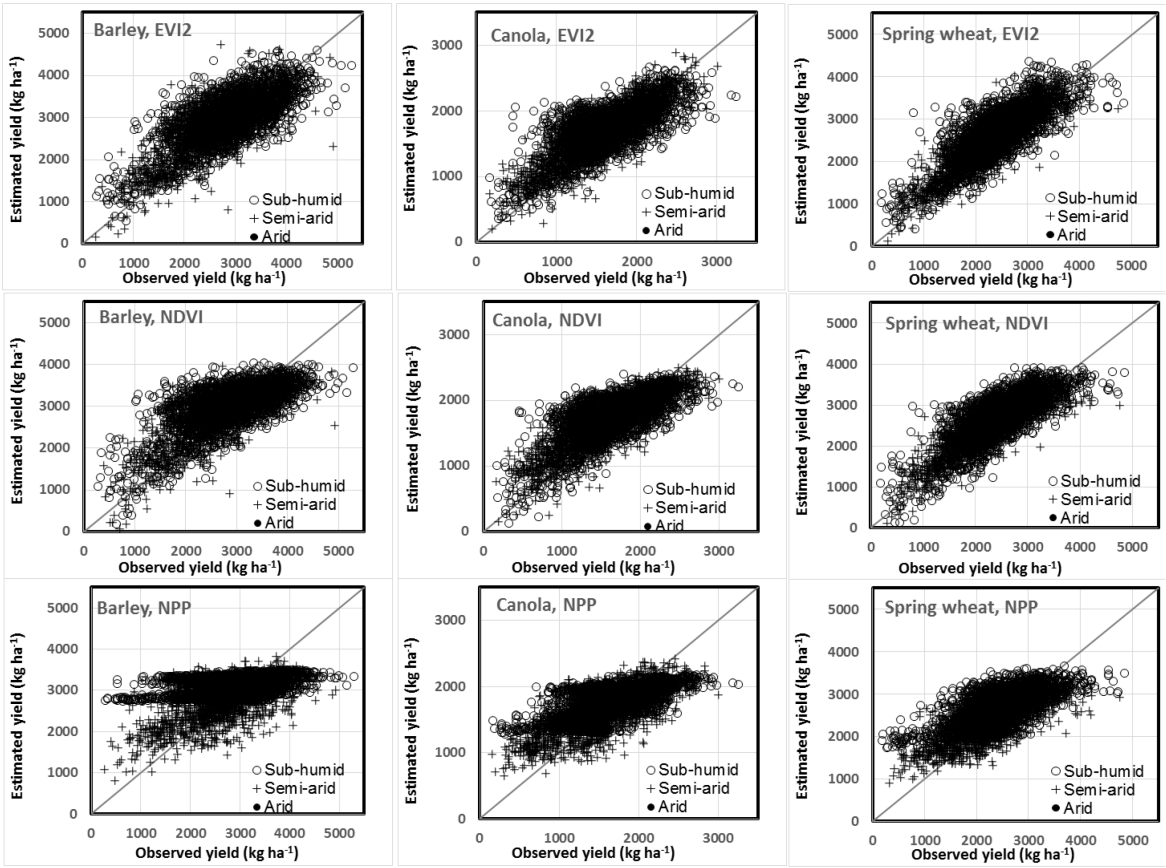

Fig. 6. Comparison of measured and estimated crop yields at Saskatchewan at the Rural Municipality (RM) level using multiple linear regression models established with CAR-level grain yields.

This study and several others showed that yield estimation can be improved through temporal smoothing of time-series vegetation indices [15], [45], [46]. This is because running averages of time-series vegetation indices can help stabilize or improve model performance by getting rid of noise in the data. Considering that crops usually remain at their peak growing stage for a period of time, maximum photosynthetic capacity can still be measured, and a simple model can be implemented for application over multiple years. In a study in the central United States, Bolton and Friedl [20] derived county-level average time-series vegetation indices using "phenologically adjusted" time-series vegetation indices for crop yield estimation at the pixel level. This adjustment relies on the detection of green-up date, whose accuracy influences final results. Identifying green-up date can be difficult when spring snow cover is present in the time-series signals of green vegetation development [47].

Fig. 2 shows that NSE of EVI2 is higher than that of NDVI during the peak growing stage, and Fig. 4 shows that the underestimation at the high yield ranges is less severe using EVI2 than using NDVI. These results agree with the previous studies showing that EVI2 is less prone to saturation at high biomass [18], [48]. As the three-band counterpart of EVI2, MODIS EVI was found to outperform other vegetation indices for GPP estimation when the indices were scaled [49]. Fig. 9 shows the relationship between CAR-level peak growing stage NDVI and EVI2. Peak growing stage NDVI is larger than EVI2, with a range from 0.54 to 0.81 in the subhumid zone, 0.42 to 0.78 in the semiarid zone, and 0.32 to 0.75 in the arid zone. The two indices are strongly correlated with an exponential model. The relative rate of increase of EVI2 over NDVI (i.e., first derivative of EVI2 as function of NDVI) is smaller than 1 at the lower range but larger than 1 at the higher range of NDVI (Fig. 9). This illustrates that EVI2 is less susceptible to saturation with increasing green biomass, and hence an increased sensitivity at higher crop yields than NDVI. Since EVI2 is also more resistant to atmospheric interference than NDVI [12], [18], it is recommended as a better predictor of crop yield.

C. GPP and NPP

Fig. 3 shows that NSE of MODIS annual cumulative GPP and NPP is comparable to that of maximum GPP. The NSE of these metrics is lower than that of peak stage EVI2 or NDVI. MODIS daily GPP is calculated as the product of the realized light use efficiency (ε), solar incident PAR, and MODIS fAPAR [39], [40]. GPP is correlated with MODIS vegetation indices since fAPAR can be considered proportional to NDVI (or EVI2). Although it incorporates meteorological constraints through temperature and moisture stresses, the peak value of GPP has a weaker determination on grain yields than peak

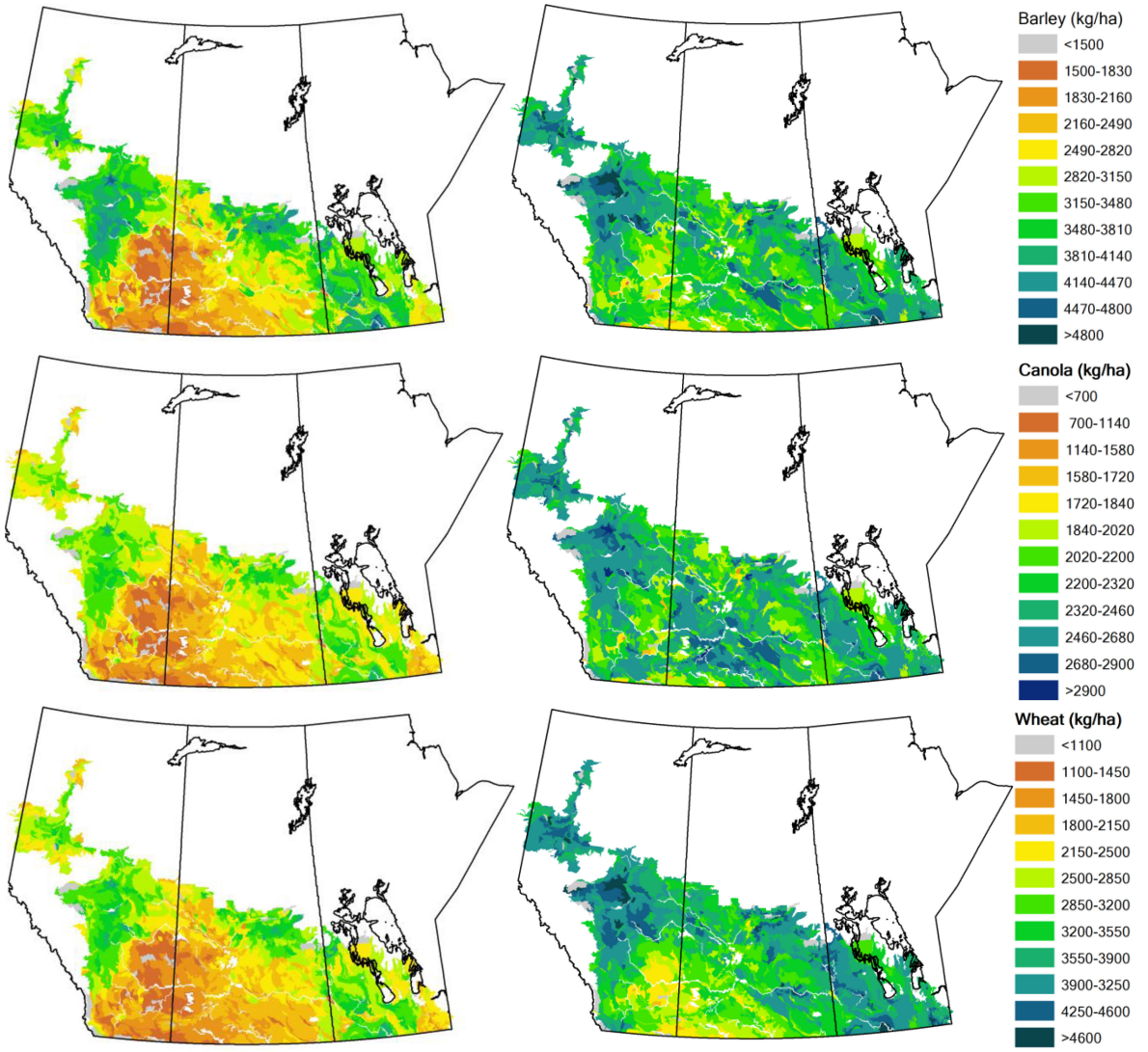

Fig. 7. Estimated crop yields in 2000 (left) and 2016 (right) for barley (top), canola (middle), and spring wheat (bottom) at the Soil Landscape of Canada level, using a regression model based on EVI2.

vegetation indices. We tested vegetation indices calculated from MODIS 500-m reflectance data (MOD09A1) and found that the correlation with crop yields is comparable to the 250-m MODIS data. Thus, the lower correlation of MODIS GPP and NPP data with crop yields is unlikely caused by the coarser spatial resolution. However, we note here that the MODIS GPP/NPP algorithm treats cropland with the same set of biome-specific parameters. In reality, different crops may have different grain formation mechanisms, and different light use efficiency [50]. Further study is necessary to improve the modeling of crop GPP and NPP for final grain yield estimation.

D. Spatiotemporal Variability

Our results show that the regression models developed from CAR-level data can be used for RM-level yield estimation with acceptable accuracy (Fig. 6 and Table. II). This indicates that 250-m peak stage MODIS EVI2 may be useful for disaggregating CAR-level grain yields for mapping yields at a finer spatial resolution. In contrast to the more cadastrally delineated RM polygons, SLC polygons delineate patterns of natural physical conditions (soils, landscape, and climate), and their boundaries are more intricate. Crop growth conditions in an SLC polygon can be obtained from time-series MODIS data if there are enough representative cropland pixels in each polygon. There are 1434 SLC polygons in the Canadian Prairies with annual cropping activities. More than 95% of the polygons have more than 50 qualified 250-m cropland pixels. Thus, it is reasonable that the model can be applied for crop grain yield mapping at the SLC level (Fig. 7) to generate a historical database across this agricultural region. However, as noted, poor model performance is shown in certain years, as shown by the spikes of large RRMSE in 2003, 2007, and 2012 (Fig. 5). The similar behavior of the models based on peak stage vegetation indices and those based on annual NPP indicates that abnormal yield-limiting effects are not successfully captured by the models. For instance, in 2012 in

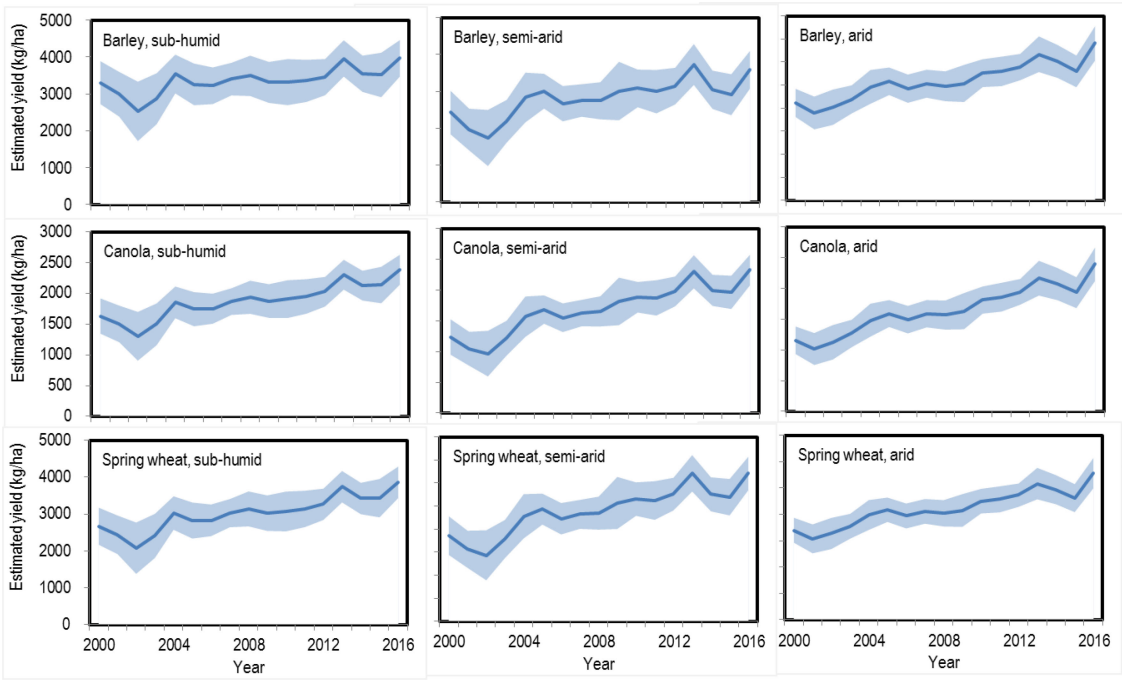

Fig. 8. Annual variation of estimated grain yields for barley (top), canola (middle), and spring wheat (bottom) in three agro-climate zones. Solid line represents the averages, and shaded band represents ± 1 standard deviations of estimated yields at the Soil Landscapes of Canada (SLC) level.

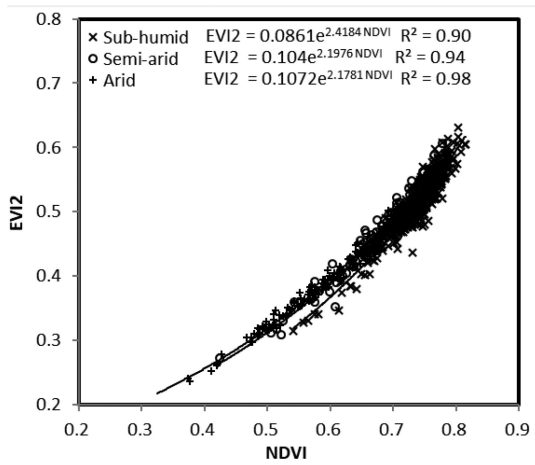

Fig. 9. Comparison of CAR-level maximum NDVI and EVI2.

Saskatchewan, flooding, heat stress, diseases, insects, wind, and hail influenced the growth of many crops across the province[4]. Here, the eastern prairies experienced excessive moisture, while the southern prairies experienced high temperatures and heat stress. Yield estimation models based on remotely sensed vegetation indices may benefit from incorporating these extreme conditions.

V. Conclusion

The use of MODIS data for estimating grain yields of barley, canola, and spring wheat in the Canadian Prairies was evaluated at two spatial scales. Correlations between crop yields and MODIS vegetation indices show clear seasonal patterns, with the strongest correlations being observed at peak growth in late July and early August. EVI2 was observed to be better than NDVI for crop yield estimation, and a running average with three 8-day composites improves model performance. The correlation between crop yields and MODIS GPP or NPP is lower than that between crop yield and peak growing stage vegetation indices. A multiple linear regression model can be established for crop yield estimation, using MODIS data to reveal spatiotemporal variability of crop productivity and to identify long term yield trends. Using seasonal maximum EVI2 as a predictor, the relative root-mean-square-error of estimation is between 14% and 20% for the three crops in the three agro-climate zones, and the respective coefficients of determination are between 0.53 and 0.70. Although interannual variation exists, leave-one-out cross validation demonstrated model stability and robustness across different years. Model evaluation using crop yield data at a finer spatial resolution showed its applicability to disaggregating crop yields from a coarser resolution to finer spatial resolutions. This study provides a potential approach for establishing a long term historical crop yield database across the Canadian Prairies.

[4]http://www.agriculture.gov.sk.ca/Crop-Report

References

[1] Y. Zhang*et al.*, "Effect of using crop specific masks on earth observation based crop yield forecasting across Canada," *Remote Sens. Appl.: Soc. Environ.*, vol. 13, pp. 121–137, 2019.

[2] A. Chipanshi *et al.*, "Evaluation of the Integrated Canadian Crop Yield Forecaster (ICCYF) model for in-season prediction of crop yield across the Canadian agricultural landscape," *Agricultural Forest Meteorol.*, vol. 206, pp. 137–150, 2015.

[3] B. Wu, J. Meng, Q. Li, N. Yan, X. Du, and M. Zhang, "Remote sensing-based global crop monitoring: Experiences with China's CropWatch system," *Int. J. Digital Earth*, vol. 7, no. 2, pp. 113–137, 2014.

[4] R. L. Clearwater, T. Martin, and T. Hoppe, "Environmental sustainability of Canadian agriculture: Agri-environmental indicator report series" Agriculture and Agri-Food Canada, Ottawa, ON, Canada, Rep. 4, 2016.

[5] X. Li, E. Mupondwa, S. Panigrahi, L. Tabil, S. Sokhansanj, and M. Stumborg, "A review of agricultural crop residue supply in Canada for cellulosic ethanol production," *Renewable Sustain. Energy Reviews*, vol. 16, no. 5, pp. 2954–2965, 2012.

[6] R. Alvarez, "Predicting average regional yield and production of wheat in the Argentine Pampas by an artificial neural network approach," *Eur. J. Agronomy*, vol. 30, no. 2, pp. 70–77, 2009.

[7] A. K. Prasad, L. Chai, R. P. Singh, and M. Kafatos, "Crop yield estimation model for Iowa using remote sensing and surface parameters," *Int. J. Appl. Earth Observation Geoinformation*, vol. 8, no. 1, pp. 26–33, 2006.

[8] B. Qian, R. De Jong, R. Warren, A. Chipanshi, and H. Hill, "Statistical spring wheat yield forecasting for the Canadian Prairie provinces," *Agricultural Forest Meteorol.*, vol. 149, no. 6, pp. 1022–1031, 2009.

[9] J. M. Chen *et al.*, "Derivation and validation of Canada-wide coarse-resolution leaf area index maps using high-resolution satellite imagery and ground measurements," *Remote Sens. Environ.*, vol. 80, no. 1, pp. 165–184, 2002.

[10] A. A. Gitelson, Y. J. Kaufman, R. Stark, and D. Rundquist, "Novel algorithms for remote estimation of vegetation fraction," *Remote Sens. Environ.*, vol. 80, no. 1, pp. 76–87, 2002.

[11] J. Liu, J. R. Miller, D. Haboudane, E. Pattey, and K. Hochheim, "Crop fraction estimation from casi hyperspectral data using linear spectral unmixing and vegetation indices," *Canadian J. Remote Sens.*, vol. 34, pp. S124–S138, 2008.

[12] J. Liu, E. Pattey, and G. Jégo, "Assessment of vegetation indices for regional crop green LAI estimation from Landsat images over multiple growing seasons," *Remote Sens. Environ.*, vol. 123, pp. 347–358, 2012.

[13] F. Gao, M. Anderson, C. Daughtry, and D. Johnson, "Assessing the variability of corn and soybean yields in central iowa using high spatiotemporal resolution multi-satellite imagery," *Remote Sen.*, vol. 10, 2018, Art. no. 1489.

[14] D. M. Johnson, "An assessment of pre- and within-season remotely sensed variables for forecasting corn and soybean yields in the United States," *Remote Sens. Environ.*, vol. 141, pp. 116–128, 2014.

[15] M. S. Mkhabela, P. Bullock, S. Raj, S. Wang, and Y. Yang, "Crop yield forecasting on the Canadian Prairies using MODIS NDVI data," *Agricultural Forest Meteorol.*, vol. 151, no. 3, pp. 385–393, 2011.

[16] A. Huete, K. Didan, T. Miura, E. P. Rodriguez, X. Gao, and L. G. Ferreira, "Overview of the radiometric and biophysical performance of the MODIS vegetation indices," *Remote Sens. Environ.*, vol. 83, no. 1/2, pp. 195–213, 2002.

[17] A. R. Huete, H. Q. Liu, K. Batchily, and W. Van Leeuwen, "A comparison of vegetation indices over a global set of TM images for EOS-MODIS," *Remote Sens. Environ.*, vol. 59, no. 3, pp. 440–451, 1997.

[18] Z. Jiang, A. Huete, K. Didan, and T. Miura, "Development of a two-band enhanced vegetation index without a blue band," *Remote Sen. Environ.*, vol. 112, no. 10, pp. 3833–3845, 2008.

[19] I. Becker-Reshef, E. Vermote, M. Lindeman and C. Justice, "A generalized regression-based model for forecasting winter wheat yields in Kansas and Ukraine using MODIS data," *Remote Sens. Environ.*, vol. 114, no. 6, pp. 1312–1323, 2010.

[20] D. K. Bolton and M. A. Friedl, "Forecasting crop yield using remotely sensed vegetation indices and crop phenology metrics," *Agricultural Forest Meteorol.*, vol. 173, pp. 74–84, 2013.

[21] B. C. Gao, "NDWI–A normalized difference water index for remote sensing of vegetation liquid water from space," *Remote Sens. Environ.*, vol. 58, no. 3, pp. 257–266, 1996.

[22] T. Dong *et al.*, "Estimating winter wheat biomass by assimilating leaf area index derived from fusion of Landsat-8 and MODIS data.," *Int. J. Appl. Earth Observation Geoinformation*, vol. 49, pp. 63–74, 2016.

[23] C. Liao, J. Wang, I. Pritchard, J. Liu, and J. Shang, "A spatio-temporal data fusion model for generating NDVI time series in heterogeneous regions," *Remote Sens.*, vol. 9, no. 11, 2017, Art. no. 1125.

[24] W. G. M. Bastiaanssen and S. Ali, "A new crop yield forecasting model based on satellite measurements applied across the Indus Basin, Pakistan," *Agriculture, Ecosystems Environ.*, vol. 94, no. 3, pp. 321–340, 2003.

[25] J. Liu, E. Pattey, J. R. Miller, H. McNairn, A. Smith, and B. Hu, "Estimating crop stresses, aboveground dry biomass and yield of corn using multi-temporal optical data combined with a radiation use efficiency model," *Remote Sens. Environ.*, vol. 114, no. 6, pp. 1167–1177, 2010.

[26] X. Xiao *et al.*, "Satellite-based modeling of gross primary production in an evergreen needleleaf forest," *Remote Sens. Environ.*, vol. 89, no. 4, pp. 519–534, 2004.

[27] X. Xiao, Q. Zhang, D. Hollinger, J. Aber, and M. Berrien Iii, "Modeling gross primary production of an evergreen needleleaf forest using modis and climate data," *Ecological Appl.*, vol. 15, no. 3, pp. 954–969, 2005.

[28] M. Zhao and S. W. Running, "Drought-induced reduction in global terrestrial net primary production from 2000 through 2009 (Science (1093))," *Science*, vol. 334, no. 6062, 2011, Art. no. 1496.

[29] S. D. Prince and S. N. Goward, "Global primary production: a remote sensing approach," *J. Biogeography*, vol. 22, no. 4/5, pp. 815–835, 1995.

[30] C. S. Potter *et al.*, "Terrestrial ecosystem production: A process model based on global satellite and surface data," *Global Biogeochemical Cycles*, vol. 7, no. 4, pp. 811–841, 1993.

[31] G. Jégo, E. Pattey, and J. Liu, "Using Leaf Area Index, retrieved from optical imagery, in the STICS crop model for predicting yield and biomass of field crops," *Field Crops Res.*, vol. 131, pp. 63–74, 2012.

[32] L. Dente, G. Satalino, F. Mattia, and M. Rinaldi, "Assimilation of leaf area index derived from ASAR and MERIS data into CERES-Wheat model to map wheat yield," *Remote Sens. Environ.*, vol. 112, no. 4, pp. 1395–1407, 2008.

[33] B. Duchemin, P. Maisongrande, G. Boulet, and I. Benhadj, "A simple algorithm for yield estimates: Evaluation for semi-arid irrigated winter wheat monitored with green leaf area index," *Environmental Modelling Softw.*, vol. 23, no. 7, pp. 876–892, 2008.

[34] Ecological Stratification Working Group, *A National Ecological Framework for Canada*, 1995.

[35] S. M. McGinn, "Weather and Climate Patterns in Canada's Prairie Grasslands," in *Arthropods of Canadian Grasslands: Ecology and Interactions in Grassland Habitats*, J. D. Shorthouse, and K. D. Floate, Eds., Ottawa, ON, USA: Biological Survey of Canada, 2010, ch. 5, pp. 105–119.

[36] J. Shang *et al.*, "Mapping spatial variability of crop growth conditions using RapidEye data in Northern Ontario, Canada," *Remote Sens. Environ.*, vol. 168, pp. 113–125, 2015.

[37] J. D. White, N. A. Scott, A. I. Hirsch, and S. W. Running, "3-PG productivity modeling of regenerating Amazon forests: Climate sensitivity and comparison with MODIS-derived NPP," *Earth Interact.*, vol. 10, no. 8, pp. 1–26, 2006.

[38] J. L. Monteith, "Solar radiation and productivity in tropical ecosystems," *J. Appl. Ecology*, vol. 9, no. 3, pp. 747–766, 1972.

[39] S. Running, Q. Mu, and M. Zhao, "MOD17A2H MODIS/Terra gross primary productivity 8-Day L4 Global 500m SIN Grid V006," NASA EOSDIS Land Processes DAAC, 2015, doi: 10.5067/MODIS/MOD17A2H.006.

[40] S. Running, Q. Mu, and M. Zhao, "MOD17A3H MODIS/Terra Net Primary Production Yearly L4 Global 500m SIN Grid V006," NASA EOSDIS Land Processes DAAC, 2015, doi: 10.5067/MODIS/MOD17A3H.006.

[41] M. Zhao, F. A. Heinsch, R. R. Nemani, and S. W. Running, "Improvements of the MODIS terrestrial gross and net primary production global data set," *Remote Sens. Environ.*, vol. 95, no. 2, pp. 164–176, 2005.

[42] T. Huffman, M. Olesen, M. Green, D. Leckie, J. Liu, and J. Shang, "Agricultural data analytics for environmental monitoring in Canada," *Federal Data Science*, F. A. Batarseh and R. Yang, Eds., San Francisco, CA, USA: Academic Press, 2018, ch. 5, pp. 55–79.

[43] T. O. Kvålseth, "Cautionary note about R^2," *Amer. Statistician*, vol. 39, no. 4, pp. 279–285, 1985.

[44] A. M. Davidson, T. Fisette, H. McNairn, and B. Daneshfar, "Detailed crop mapping using remote sensing data (crop data layers)," *Handbook on Remote Sensing for Agricultural Statistics*. J. Delincé, Ed., Rome: Global Strategy Improving Agricultural and Rural Statistics (GSARS), ch. 4, 2017. [Online]. Available: http://gsars.org/wp-content/uploads/2017/09/GS-REMOTE-SENSING-HANDBOOK-FINAL-04.pdf

[45] M. S. Mkhabela, M. S. Mkhabela, and N. N. Mashinini, "Early maize yield forecasting in the four agro-ecological regions of Swaziland using NDVI data derived from NOAA's-AVHRR," *Agricultural Forest Meteorol.*, vol. 129, no. 1/2, pp. 1–9, 2005.

[46] K. P. Hochheim and D. G. Barber, "Spring wheat yield estimation for Western Canada using NOAA NDVI data," *Can. J. Remote Sens.*, vol. 24, pp. 17–27, 1998.

[47] N. Delbart, T. Le Toan, L. Kergoat, and V. Fedotova, "Remote sensing of spring phenology in boreal regions: A free of snow-effect method using NOAA-AVHRR and SPOT-VGT data (1982–2004)," *Remote Sens. Environ.*, vol. 101, no. 1, pp. 52–62, 2006.
[48] J. Shang *et al.*, "Estimating plant area index for monitoring crop growth dynamics using Landsat-8 and RapidEye images," *J. Appl. Remote Sens.*, vol. 8, 2014, Art. no. 085196.
[49] Q. Zhang *et al.*, "Estimation of crop gross primary production (GPP): II. Do scaled MODIS vegetation indices improve performance?" *Agricultural Forest Meteorol.*, vol. 200, pp. 1–8, 2015.
[50] Q. Xin, M. Broich, A. E. Suyker, L. Yu, and P. Gong, "Multi-scale evaluation of light use efficiency in MODIS gross primary productivity for croplands in the midwestern United States," *Agricultural Forest Meteorol.*, vol. 201, pp. 111–119, 2015.

Jiangui Liu received the bachelor's degree in electronics engineering from Tsinghua University, Beijing, China, in 1990, and the Ph.D. degree in cartography and remote sensing from the Chinese Academy of Sciences, Beijing, in 1999.

He is currently a Physical Scientist with the Science and Technology Branch, Agriculture and Agri-Food Canada, Ottawa, ON, Canada. His research interests include remote sensing for crop and soil biophysical parameters estimation, crop productivity modeling, and agri-environmental sustainability assessment.

Ted Huffman received the B.Sc. degree in resource management from the University of Guelph, Guelph, ON, Canada, in 1974, the M.A. degree in geography from Carleton University, Ottawa, ON, Canada, in 1983, and the Ph.D. degree in remote sensing from the University of Waterloo, Waterloo, ON, Canada, in 1993.

He is a Research Scientist with the Science and Technology Branch of Agriculture and Agri-Food Canada, Ottawa, ON, Canada. His research interests include the integration of earth observation with other spatial data in the development of new procedures and data for agri-environmental applications.

Budong Qian received the B.S. degree from Nanjing Institute of Meteorology, Nanjing, China, in 1982 and M.Sc. degree from Hohai University, Nanjing, China, in 1990. He received the Ph.D. degree in physics (meteorology) from the University of Lisbon, Lisbon, Portugal, in 1999.

He is currently a Research Scientist with Agriculture and Agri-Food Canada, Ottawa, ON, Canada. His research interests include impacts of climate variability and change on agricultural production and food security and development of adaptation strategies to climate change.

Jiali Shang received the B.Sc. degree in geography from Beijing Normal University, Beijing, China, in 1984, the M.A. degree from the University of Windsor, Windsor, ON, Canada, in 1996, and the Ph.D. degree in remote sensing from the University of Waterloo, Waterloo, ON, in 2005.

She is currently a Research Scientist with the Science and Technology Branch of Agriculture and Agri-Food Canada, Ottawa, ON, Canada. She is involved in the method development of optical and radar integration for agriculture applications.

Qingmou Li received the bachelor's and master's degrees in geophysics from Changchun University of Earth Sciences, Changchun, China, in 1986 and 1989, and Ph.D. degree in natural resource prospecting from China University of Geoscience, Beijing, China, in 1994.

He is currently a Research Scientist with the Space Weather Center, Canada Hazards Information Service (CHIS), Natural Resources Canada, Ottawa, ON, Canada. His research interests include using remote sensing for hazards mapping, geophysical data modeling/inversion, and machine learning for natural resources assessment.

Taifeng Dong received the bachelor's degree in geographic information system from Central South University, Changsha, Hunan, China, in 2008, and the Ph.D. degree in cartography and remote sensing from the Institute of Remote Sensing and Digital Earth, Chinese Academy of Sciences, Beijing, China, in 2013.

He is currently a Postdoctoral Fellow with the Science and Technology Branch of Agriculture and Agri-Food Canada, Ottawa, ON, Canada. His research interests include crop biophysical variable estimation, crop phenology/productivity modeling, RS data assimilation with crop growth models, and climate change impacts on agriculture assessment using remote sensing.

Andrew Davidson received the B.Sc degree from the Institute of Geography from the University of Edinburgh, Edinburgh, Scotland, in 1993, and the M.Sc and the Ph.D. degrees from the Department of Geography at the University of Toronto, Toronto, ON, Canada, in 1995 and 2002, respectively.

He is currently the Manager of Earth Observation in Agriculture Canada's Centre for AgroClimate, Geomatics and Earth Observation (ACGEO). He is also an Adjunct Research Professor with the Department of Geography and Environmental Studies at Carleton University, Ottawa, ON, Canada.

Dr. Davidson is a Fellow of the Royal Canadian Geographic Society (RCGS), since 2013.

Qi Jing received the B.Sc. and M.Sc. degrees in agronomy from Nanjing Agricultural University, Nanjing, China, in 1998 and 2001, respectively, and the Ph.D. degree in crop science from the Wageningen University and Research Centre, Wageningen, The Netherlands, in 2007, with a focus on production ecology and resource conservation.

He was a Teacher and a Researcher with the Nanjing Agricultural University. He worked as a Postdoctor at the Plant Research International in Wageningen University, at the Quebec Research and Development Centre in Agriculture and Agri-Food Canada, and Natural Science and Engineering Research Council of Canada. In 2016, he joined in the Ottawa Research and Development Centre, Agriculture and Agri-Food Canada, Ottawa, ON, Canada. His research interests include modeling plant-soil systems for annual and perennial crops, crop ecophysiology, and crop husbandry.